A 10Gb/s Mach-Zehnder Silicon Evanescent Modulator

Hui-Wen Chen, Ying-hao Kuo, and John E. Bowers

Department of Electrical and Computer Engineering, University of California Santa Barbara, Santa Barbara, CA 93106
hwchen@ece.ucsb.edu

Abstract

We demonstrate a 10 Gb/s Mach-Zehnder silicon evanescent modulator utilizing coplanar waveguide design. The device has a modulation efficiency of 1.5V-mm and modulation bandwidth of 8 GHz.

I. Introduction

Recently, silicon photonics has drawn considerable attention due to its potential for low cost manufacturing through the use of standard CMOS process. Silicon modulators are of great interest for implementing high speed optical communication systems. Several approaches have been demonstrated in order to achieve this goal. A Mach-Zehnder modulator (MZM) utilizing carrier depletion inside the silicon waveguides operating up to 40 Gb/s has been demonstrated with a modulation efficiency of 40 V-mm [1]. Ring resonator structures are more compact and have been demonstrated with speed up to 12.5 Gb/s using pre-emphasis electrical signals [2], but have a narrow optical bandwidth. To overcome the trade offs between modulation efficiency and high speed performance, an electroabsorption modulator (EAM) was demonstrated on the silicon evanescent platform with 10 dB extinction ratio (ER) at bias at -5 V, 16 GHz modulation bandwidth and 30 nm optical bandwidth [3]. Another approach to simultaneously achieve high speed operation, low voltage drive and large optical bandwidth (~100nm), is a MZM utilizing carrier depletion in offset multiple quantum wells (MQW) [4]. The carrier depletion effect is more practical for high speed application since it is not limited by carrier life time (~ns), which is an issue for devices using carrier injection. In this work, we successfully demonstrate a high speed MZM with record low modulation efficiency for a wide optical bandwidth. This modulator can be integrated with distributed Bragg reflector (DBR) lasers to generate data streams at multiple wavelengths, and thus can be applied in a WDM system. Moreover, the modulator can also be used for switch arrays.

II. Device Design and Fabrication

The MZM is fabricated on the hybrid silicon platform [5]. Both the separate confinement heterostructure (SCH) layer and MQW are intentionally doped to introduce free carriers. Unlike conventional bulk III-V diode structure, the MQW structure utilizes the change of fundamental states in the MQW rather than the change of the depletion width when small bias voltage is applied [6]. As the bias increases, the fundamental state of each QW moves and consequently results in the depletion of carriers. Hence it can produce greater modulation efficiency compared to bulk III-V and silicon material at a given bias.

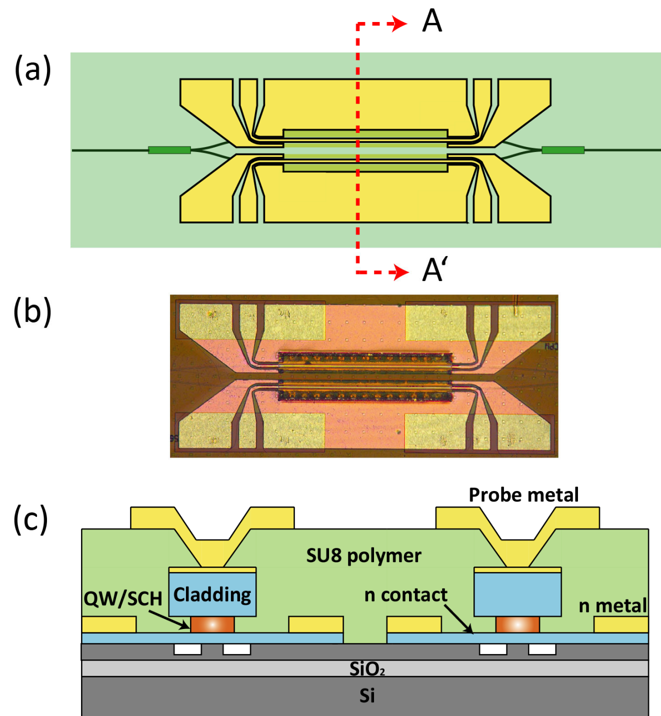

Figure 1: (a) Top view of a device with a CPW electrode (b) The optical image of the device under microscope (c) Cross section (along A-A') of the hybrid waveguide.

The top view of a 500 µm MZM is shown in Fig.1 (a). It has two MMIs, each 6 µm wide and 40 µm long, at the input and output functioning as the splitter and the combiner. Due to mode mismatch between the passive and hybrid sections, two 60 µm long tapers are added to minimize reflection and increase coupling efficiency. In addition, we use coplanar waveguides (CPW) as the traveling-wave electrode to achieve high speed performance. The optical image of a fabricated device is also shown in Fig.1 (b). A thin layer of silicon nitride, shown as orange cross region in the figure, is deposited at the end of the process to protect device from scratches. Fig.1 (c) illustrates the cross section of a MZM. The device has a 4 µm cladding width while the QW/SCH layers are under-cut to 2µm to reduce the device capacitance. The two arms of the

978-1-4244-1768-1/08/$25.00©2008 IEEE

MZM are electrically isolated by etching down the n-contact layer in between. The silicon waveguides have a height of 0.46 μm, a slab height of 0.19 μm, and a width of 0.94 μm.

The modulators are fabricated using a standard process of making silicon evanescent devices [7]. The III-V epitaxial layers are first bonded to a silicon-on-insulator wafer by using vertical outgassing channel (VOC) technique with an anneal time of 3 hours at 300°C [8]. The substrate is then removed and ready for lithographic based fabrication. In order to align contact metal with narrow width of the cladding layer, the cladding mesa are formed by using a self-aligned dry etch process. The sample is then dipped into a mixture of $H_2O/H_2O_2/H_3PO_4$ to create the under-cut in the MQW/SCH layers, while a circular pattern is used as a reference to monitor the etching distance. Next, all III-V epitaxial layers are removed on top of passive regions, and a 1 μm n-metal is deposited to form the ground metal of the CPW. A 5 μm thick polymer is then applied to provide additional mechanical support to the thin bonding layer and to separate the probe metal from the bottom n-metal in order to implement the desired CPW design and reduce parasitic capacitances.

III. Experimental Results

To test the MZM, lensed fibers are used at both ends of the chip to couple the light in and out of the anti-reflection coated silicon waveguide. The normalized transmission as a function of reverse bias with different bias at the other arm is shown in Fig.2. As can be seen, it indicates a modulation efficiency of 1.5 V-mm. The extinction ratio (ER) with the bias of 0 V and -1.6 V at the other arm are 8.65 dB and 11.6 dB, respectively. The difference of ER is due to the loss imbalance introduced between two arms since the quantum-confined Stark effect (QCSE) becomes more significant while applied voltage is greater than 3V.

The high speed performance of this device was explored as well. The electrical S21, displayed in Fig.3 in the black curve, was first measured using an Agilent 8164A PNA

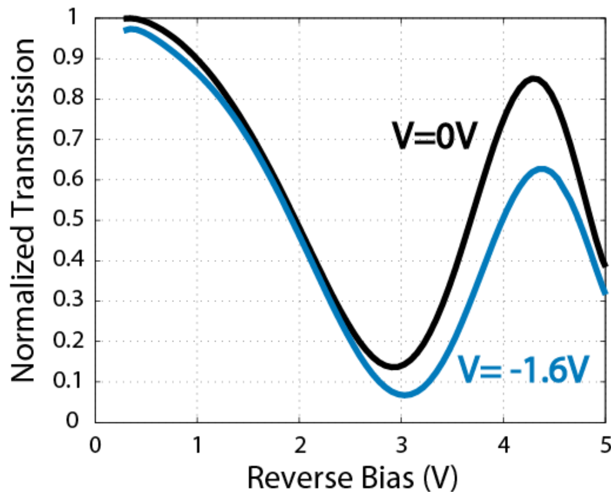

Figure 2: Modulation efficiency of a 500 μm device with different bias at the other arm at 1550 nm.

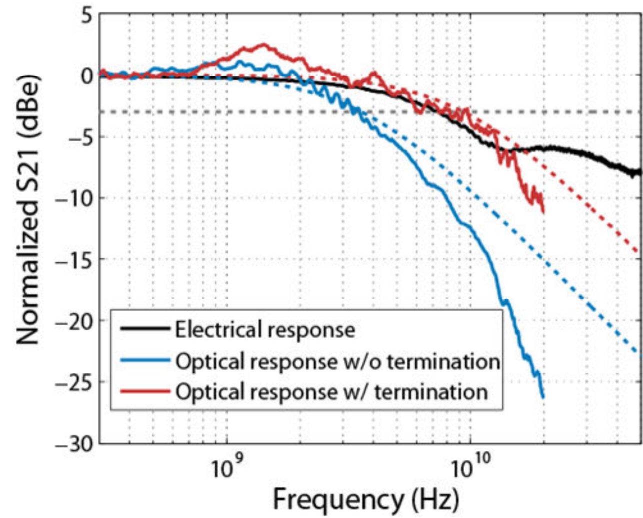

Figure 3: Experimental electrical and optical response together with estimated RC limited curves.

network analyzer. By extracting full 4-port S parameters, the characteristic impedance of 20 Ω and the electrical propagation loss of 5 dB/mm at 10 GHz can be calculated. The experimental data depicts a 3dBe cutoff frequency at 7.5 GHz. Meanwhile, two curves of optical modulation are also exhibited in Fig.3. The response without any impedance termination at the end the CPW (blue curve) has a 3dBe cutoff frequency at 3.5 GHz, which is consistent with the estimated RC response (blue dash curve). The degradation of high speed performance is due to the large reflection from the open end of the CPW. The reflection, however, can be reduced by applying a 25 Ω termination so that the cutoff frequency can increase to 8 GHz, sufficient for 10 Gb/s data transmission.

To characterize the large signal response, a 2^{31}-1 pseudorandom bit sequence (PRBS) pattern generator connected to an electrical amplifier is used to provide the drive signal. The device is biased at -3.8 V with 3 V swing while the bias at other arm is adjusted to achieve best signal quality. The modulated light is then collected by a lensed fiber

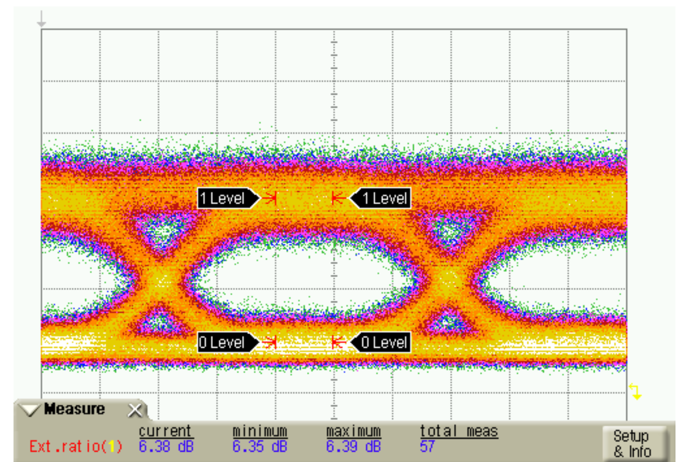

Figure 4: 10 Gb/s eye diagram with 2^{31}-1 PRBS.

and amplified with an EDFA. A filter is used to eliminate the ASE noise before the signal transmitted to an Agilent digital communication analyzer (DCA). The signal has a an ER of 6.3 dB, which is slightly smaller than the ER measured at DC bias due to the partial voltage drop on series resistance and cladding layer. The eye closure is similar at 1 Gb/s, indicating low frequency cutoff components in the measurement system.

IV. Conclusions

A silicon evanescent MZM with modulation efficiency of 1.5 V-mm is demonstrated. The modulated signal has an open eye diagram at 10 Gb/s with a ER of 6.3 dB. The demonstrated device can be used for high speed on-chip optical interconnects.

The authors acknowledge financial support from DARPA/MTO, Army, and ARL. The authors thank J. Shah, M. Haney, Alex Fang, Matt Sysak, Matt Dummer, Anand Ramaswamy and Di Liang for useful discussions.

V. References

[1] A. Liu, *et al.*, "High-speed optical modulation based on carrier depletion in a silicon waveguide," *Opt Express* **15**, 660-668(2007).
[2] Q. Xu, *et al.*, "Micrometer-scale silicon electrooptic modulator," *Nature* **435**, 325-327 (2005).
[3] Y.-H. Kuo, *et al.*, "A hybrid silicon evanescent electroabsorption modulator," *Optical Fiber Communication Conference*, San Diego, CA, 2008.
[4] H.-W. Chen, *et al.*, "Hybrid silicon evanescent phase modulator based on carrier depletion in offset multiple quantum," *Conference on Lasers and Electro-Optics*, San Jose, CA, 2008.
[5] A. W. Fang, *et al.*, "Electrically pumped hybrid AlGaInAs-silicon evanescent laser," *Opt. Express* **14**, 9203-9210 (2006).
[6] H. Ohe, *et al.,* "InGaAlAs Multiple-Quantum-Well Optical Phase Modulators Based on Carrier Depletion," *IEEE Photon. Techno. Lett* **19**, 1816–-1818 (2007)
[7] H. Park, *et al.*, "A hybrid AlGaInAs-silicon evanescent preamplifier and photodetector," *Opt. Express* **15**, Issue 21, 13539-13546 (2007).
[8] D. Liang, *et al.*, "Highly Efficient Vertical Outgassing Channels for Robust, Void-Free, Low-Temperature Direct Wafer Bonding," *The 35th Conference on the Physics and Chemistry of Semiconductor Interfaces*, Santa Fe, NM, 2008.